

Design Considerations and Deployment Simulations of Spinning Space Webs

Mattias Gärdsback* and Gunnar Tibert†

KTH Mechanics, Royal Institute of Technology, SE-100 44 Stockholm, Sweden.

Dario Izzo‡

Advanced Concepts Team, EUI-ACT, ESTEC, Keplerlaan 1, 2201 AZ Noordwijk, The Netherlands.

ESA Advanced Concepts Team (ACT) has proposed to construct large space antennas and solar power systems by deploying and stabilising a large web in space. The idea originates from the Japanese “Furoshiki Satellite”. Since an overly complicated control system contributed to the partly chaotic deployment, ACT suggests to use centrifugal forces to deploy the space web.

In this study the design and folding pattern of space webs are discussed. An analytical model and a finite element model used to describe the deployment, from the chosen folding, are presented. Free deployment of space webs is studied and a first control strategy that enables controlled and stable deployment is suggested.

I. Introduction

Power generation (solar panels), propulsion (solar sails) and communication (antennas) are examples of applications in space that require large deployable structures. Space webs can be seen as an intermediate step between today's rigid deployable structures and future deployable gossamer structures. The idea originates from the Japanese “Furoshiki Satellite”.¹⁻³ The space web is composed of a large membrane or net held in tension by thruster controlled corner satellites or by spinning the whole assembly. An idea put forward by Kaya *et al.*⁴ is to build up the antenna or solar power elements by robots that crawl on the web like spiders.

The difficulty in deploying a space web in a controlled manner was shown in the partly chaotic deployment during the Furoshiki experiment in January 2006.⁵ Thus, a deployment that is easier to control is desirable. ACT has investigated the possibilities to use centrifugal forces to deploy and stabilise the web in space.^{6,7} Deployment using centrifugal forces have many advantages, e.g., the control forces can be applied to the centre hub, all the significant forces are in the plane of rotation, and both fast and slow deployment velocities are possible.

Large structures stabilised by centrifugal forces have been considered for space applications since the early 1960s when Astro Research Corporation analysed several spin-stabilised structures,⁸⁻¹¹ most notable is the Heliogyro solar sail by MacNeal,¹² and similar spin-stabilised structures are still being considered for solar sail missions.^{13,14} In Japan, spinning concepts were considered for solar sails already in the mid 1980s,¹⁵ and recently several concepts have been analysed and tested both on ground and in space.¹⁶⁻¹⁹ Nevertheless, the only successful deployment and control of a large spin-stabilised space structure is the Russian Znamya-2 experiment in 1993.²⁰

Numerical studies have been performed on the spin-stabilisation of deployed space webs.^{7,21} In this study the focus is on the deployment phase. An analytical model is developed inspired by deployment models of circular membranes.^{20,22} A finite element model is also implemented in LS-DYNA. The two models can be used to test important design parameters and control algorithms.

*PhD Student, AIAA Student Member.

†Research Associate, AIAA Member.

‡Mission Analyst, AIAA Member.

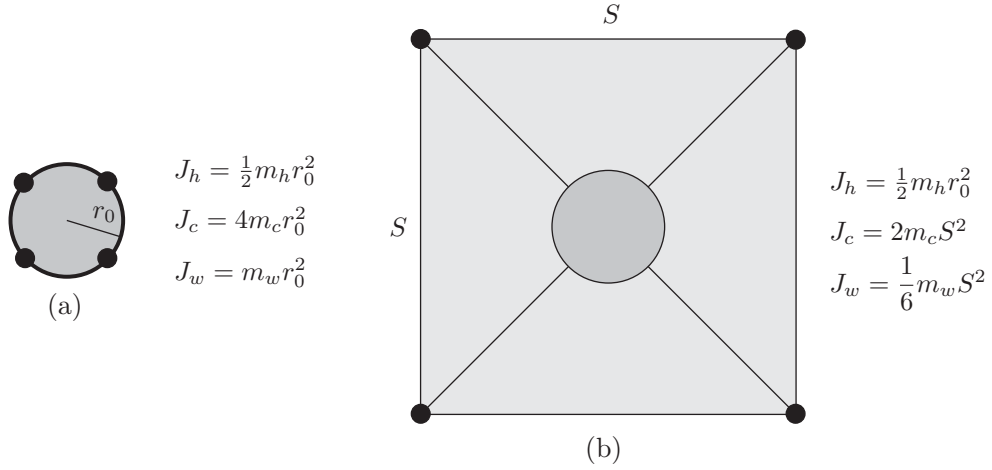


Figure 1. Moment of inertia for the system: (a) before deployment and (b) after deployment.

II. Centrifugal force deployment

The use of centrifugal forces to deploy large structures in space is appealing for many reasons:

- Spinning satellites are used for many purposes already and small-scale testing can be performed on existing satellites.
- The centrifugal force is always in the plane of rotation of the spinning satellite. Therefore, as long as the rotational forces are dominating, the out-of-plane motion will be negligible.
- For centrifugal deployment, the control is relatively simple. Increased control requires more expensive equipment, which also increases the risk of technical problems and unsuccessful deployment.
- Centrifugal force deployment can be either slow or fast, whichever leads to a controlled deployment.

A minimum of control is desirable, and preferably free deployment where the membrane or web is deployed from the initial rotation of the satellite without any control. However, two fundamental physical laws, the conservation of angular momentum and conservation of energy, makes this difficult. The total angular momentum K must be constant, i.e.

$$K = J_0 \omega_0 = J_f \omega_f \quad (1)$$

where J is the moment of inertia, ω is the angular velocity of the system and indices 0 and f denotes the initial and the final states, respectively. At the same time the energy E must be constant:

$$E = \frac{J_0 \omega_0^2}{2} = \frac{J_f \omega_f^2}{2} + E_{\text{surplus}} \quad (2)$$

Since the moment of inertia, Figure 1, and consequently the angular momentum, increases with the square of the size of the deployed structure, from the small stowed size r_0 to the much greater deployed side length S , the angular velocity must decrease at the same rate. For free deployment, this implies low final angular velocities for very large structures, and that almost all the initial kinetic energy must be removed somehow. Otherwise, the surplus of energy will cause oscillations in the plane of rotation.

Webs also have a tendency to get entangled, but the risk of entanglement decreases substantially if the space web is not coiled back on the central satellite. Hence, to obtain a successful centrifugal deployment of a space web, the first task is to find a folding pattern and a robust control law that enable this.

III. Web design

Prior studies^{4,5} have not looked into the various choices of web geometry and mesh topology. The prestress distribution in the web is not uniform due to the centrifugal force field and it is required that the

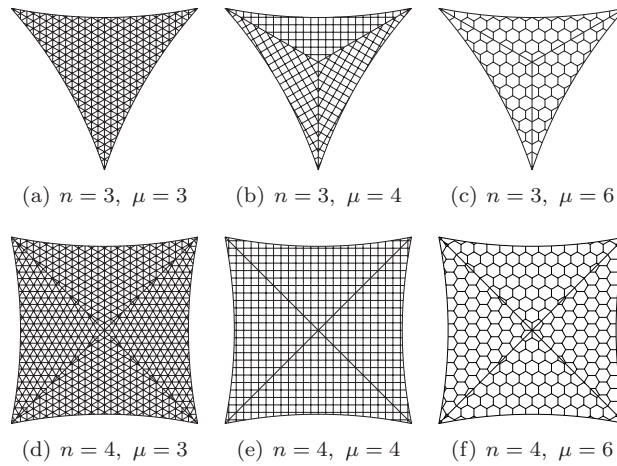


Figure 2. Possible web and mesh configurations for $n = 3, 4$ and $\mu = 3, 4, 6$.

web is in tension everywhere. The prestress in the web provides the out-of-plane stiffness and that stiffness may depend on the choice of mesh topology. The spinning of the web and the low out-of-plane stiffness create undesirable dynamic phenomena, such as travelling waves and excess out-of-plane deformations, which affect the performance of the web. Due to all these aspects, a thorough analysis is required to obtain an adequate design of the web.

Web material

The web should be manufactured from a very light, but strong and stiff material. As the Zylon[®] fibre has superior properties compared to other fibres,^{23,24} Zylon[®] is the preferred choice for manufacturing the space web.⁶ However, like most high performance fibres, Zylon[®] suffers from strength degradation when exposed to light.²³⁻²⁵

Web geometry and topology

Six possible space web configurations with triangular, quadratic and hexagonal mesh topologies and three and four corners, Figure 2, have been investigated.⁶ In terms of manufacturing, the most regular web configurations are:

- Triangular web and triangular mesh (TriTri).
- Triangular web and hexagonal mesh (TriHex).
- Quadratic web and quadratic mesh (QuadQuad).

The optimum layout of the web is determined by the following parameters: (i) prestressability (ii) manufacturability, (iii) mass, (iv) out-of-plane stiffness and (v) eigenfrequencies, but not necessarily in that order. Analysis using the force method^{26,27} shows that only the quadratic mesh is prestressable by centrifugal forces.⁶ A quadratic web with a quadratic mesh is better from a manufacturing viewpoint and the out-of-plane stiffness and eigenfrequencies can be adjusted by the angular velocity and corner masses.⁶ The remainder of this report will thus only be concerned with the quadratic web with a quadratic mesh.

It should be noted that Schuerch and Hedgepeth⁹ also chose a quadrangular mesh for their LOFT concept, although previous reports on the LOFT,^{10,28} used a triangular mesh. The reasons for finally choosing the square mesh over the triangular one were:⁹ (i) the shearing stiffness provided by the diagonal elements was not significantly greater than the stiffening effect derived from centrifugal forces; deleterious out-of-plane motions of the surface were reduced by deleting the diagonals, as vibrational energy then goes into the less harmful in-plane mode of deformation, (ii) the square mesh has the ability to undergo large shearing deformations, without requiring in-plane strains or creases in the material; characteristics important for packaging purposes.

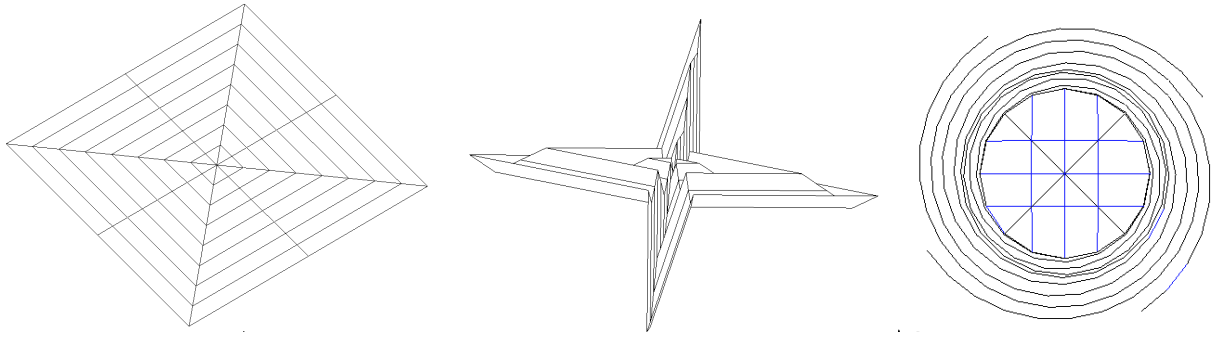


Figure 3. Complete star folding sequence for a quadratic sheet (note that not all lines are fold lines), and hub-wrapping folding of the star arms.

IV. Folding patterns for centrifugal deployment

Fundamental to a successful deployment is an appropriate folding pattern. Several folding patterns for large space structures have been proposed for various deployment approaches. A good example is the Miura-Ori²⁹ for the efficient folding of square solar sails. Several studies have dealt with the folding of a circular solar sail by wrapping it around a cylindrical hub.^{30–32} However, neither of these hub-wrapping schemes are suitable for triangular or square sheets.

Schuerch and Hedgepeth⁹ suggested a folding pattern for the LOFT system where the supporting structure is sheared to be folded into the hub. This pattern produces a star-like shape of the structure being folded. Melnikov and Koshelev²⁰ proposed a similar pattern for the folding of spin-deployed circular space structures. A similar folding pattern was also used in the experimental and numerical study of solar sail deployment by Matunaga *et al.*¹⁶

The arms of the star can then be folded in various ways.²⁰ Two approaches appear especially interesting due to their simplicity: (i) folding of the arms in a zig-zag manner towards the hub or (ii) coiling the arms around the hub as in the hub-wrapping concept.

In this study, the star pattern is preferred since it is relatively easy to control and model. For the same reasons the coiling of the arms around the hub is chosen.

V. Control

The control law should be selected so that the space web ends up in the desired configuration at the end of the deployment, within a required time period and with no undesirable oscillations or entanglement of the system. A prerequisite for a stable deployment is that the centrifugal force is much greater than the Coriolis and inertial forces.²⁰

The deployment can be controlled in different ways. The control parameters could be the torque, M , the length of the star arm, L , the angular velocity of the centre hub, ω , or the force that resists the deployment of each segment, N .

Several, more or less successful, control strategies have been described in literature. Salama *et al.*¹³ linearly increase the angular velocity ω from 0 to ω_{\max} during a time period of Δt , and then keep it constant at ω_{\max} , to deploy tethers in the first step of unfolding from a star folding. They assume that the structural damping is 5%.

Melnikov and Koshelev²⁰ use the torque and the velocity of the cable being fed out as control parameters to deploy the Znamya-2 reflector. They propose increased torque as the angular velocity decreases, according to the law:

$$M = M_0 \left(1 - \frac{\omega}{\omega_0} \right) \quad (3)$$

where M_0 is the initial momentum applied to the centre hub and ω_0 is the initial angular velocity of the centre hub. Using this strategy, a high initial angular velocity, a low angular velocity in the end, short deployment time and a stable and smooth deployment without entanglement and coiling are obtained. Melnikov and Koshelev²⁰ found that a higher value of the quotient M_0/ω_0 produces a more stable deployment. A refined

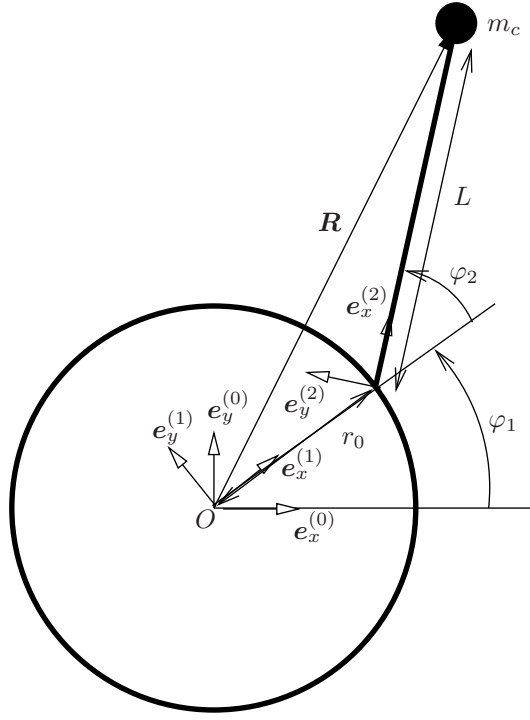


Figure 4. The analytical model for a point mass. The same coordinate systems are used for a mass distributed along the vector L .

control strategy may be necessary to compensate for, e.g., the gravity gradient.

VI. Analytical model

Simple analytical models can be used to describe the deployment dynamics qualitatively. The derivation of the equations follows the same principles used by Melnikov and Koshelev²⁰ to describe the deployment of solid reflectors and tether systems from a rotating central satellite. Hedgepeth²² also used a similar model for the LOFT system. The analytical models are based on the following assumptions:

- The star arms are straight and deployed symmetrically relative to the central axis.
- There is no out-of-plane motion.
- The gravity gradient and the elasticity in the cables are neglected.
- The energy dissipation caused by deformation, friction and environmental effects is neglected.

First the coordinate systems in Figure 4 are introduced. The equations of motion will be evaluated in system (2) where the x -axis is fixed to the tether, and the y -axis is orthogonal to the x - and the z -axis. The change in angular momentum for the central cylinder around its axis of rotation is:

$$J_z \dot{\omega} = M + nNr_0 \sin \varphi \quad (4)$$

where J_z is the moment of inertia of the centre hub around the axis of rotation z , $\omega = \dot{\varphi}_1$ is the angular velocity of the centre hub, M is the applied torque, n is the number of radial star arms or tethers, N is the tensile force in each arm/tether, r_0 is the radius of the centre hub and $\varphi = \varphi_2$ is the angle between the arm/tether and the axis from the origin to the arm/tether. For a point mass, or if the weight of the corner masses are much greater than for the web, the equations of motion become

$$m_c \left[r_0 (\omega^2 \cos \varphi - \dot{\omega} \sin \varphi) - \ddot{L} + L (\omega + \dot{\varphi})^2 \right] = N \quad (5)$$

$$m_c \left[r_0 (\dot{\omega} \cos \varphi + \omega^2 \sin \varphi) + 2(\omega + \dot{\varphi})\dot{L} + (\dot{\omega} + \ddot{\varphi})L \right] = 0 \quad (6)$$

where m_c is the corner point mass and L is the current length of the tether/arm.

Space webs folded into the star pattern can be described similarly. The deployment is performed in two steps. The dynamics of the first step, the deployment of the star arms, is most important. When the arms are deployed, the corners are approximately in position. The deployment of the rest of the web does not involve so large changes in configuration and should not pose any major problems.²⁰

The space web is first folded into n identical arms positioned symmetrically around the central hub. The arms can be folded on spools at the end of the arms, in a zig-zag pattern, or coiled around the centre hub. The line density ρ_L of an arm varies linearly, from zero at the tip of the arm. If the arm is initially coiled around the centre hub, the line density is given by

$$\rho_L = \frac{2m_w}{nH^2}(L-l) \quad (0 \leq l \leq L) \quad (7)$$

where m_w is the mass of the web and H is the length of the arm. The resulting equations of motion become

$$\frac{2m_w}{nH^2} \left[\frac{L^2}{2} \left(r_0 (\omega^2 \cos \varphi - \dot{\omega} \sin \varphi) - \ddot{L} \right) + \frac{L^3}{6} (\omega + \dot{\varphi})^2 \right] = N \quad (8a)$$

$$r_0 (\dot{\omega} \cos \varphi + \omega^2 \sin \varphi) + 2(\omega + \dot{\varphi})\dot{L} + \frac{L}{3} (\dot{\omega} + \ddot{\varphi}) = 0 \quad (8b)$$

To simulate space webs that are coiled around the centre hub, the following variable substitutions are made: $\omega = \omega + \dot{\varphi}$, $L = L - r_0 \max(0, |\varphi| - \frac{\pi}{2})$, $\dot{L} = \mp r_0 \dot{\varphi}$, $\ddot{L} = \mp r_0 \ddot{\varphi}$ and $\varphi \pm \max(|\varphi|, \frac{\pi}{2})$. Equations for many other deployment schemes can be derived similarly.⁶

VII. Finite element model

A finite element model including a centre hub, a space web and corner masses has been implemented. The node and element geometry and connectivity are generated in MATLAB. The equations of motion are then solved in LS-DYNA³³ using the explicit central difference integration method. The main differences compared to the analytical model is that perturbations can be studied, the cables can store elastic energy and the arms are not necessarily straight during the deployment.

The centre hub is modelled as a rigid body since the modelling of the coiling of the web around the centre hub is crucial. Contrary, in the corners point masses are sufficiently accurate. The cables and tethers are modelled with a great number of cable elements, i.e. truss elements with a no-compression material.

The contact between the cables and the rigid bodies, at the centre, was modelled using the kinematic constraint method.³⁴ It is not obvious how to coil the web near the hub and include contact initially. Therefore, initial contact between cable elements in the space web were disregarded, since higher priority was given to coil the space web as close to the centre hub as possible.

VIII. Results

Deployment of coiled star folded web

Quadratic space webs folded into the star pattern were shown to be of certain interest. Several different deployment simulations of a large space web with side 100 m have been performed. The following data has been used in all the simulations: the side length $S = 100$ m, the mass of the centre hub $m_h = 100$ kg, the radius of the centre hub $r_0 = 6.3$ m, the areal density of the web $\rho_A = 1.267 \cdot 10^{-2}$ kg/m² and corner mass $m_c = 10$ kg. For the FE model also the elastic modulus of the cables $E_{ca} = 180 \cdot 10^9$ Pa, the density of the cables $\rho_{ca} = 1540$ kg/m³ and the cross-sectional area of the cables $A_{ca} = 2.5/0.030 \cdot 1.23 \cdot 10^{-7}$ m² and $t = 2.5$ m were used. Note that the area is adjusted so that the total weight of the model web with 2.5 m mesh size becomes the same as for a real web with 0.030 m mesh size. In the figures where four graphs are shown, the graphs show the length of the deployed arm L , the angular deviation from the radial direction φ , the angular velocity of the inner hub ω_{centre} and the angular velocity of the tip of the arm ω_{tip} .

Free deployment of star arms

The free deployment of the star arms coiled around the centre hub was simulated, Figure 5 and 6. In Figure 6 the free deployment of the whole web is also included. During the coiling off the two curves from the two

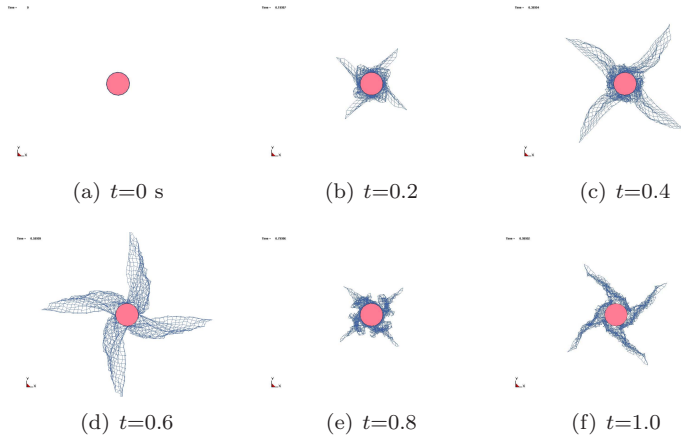


Figure 5. Free deployment of space web.

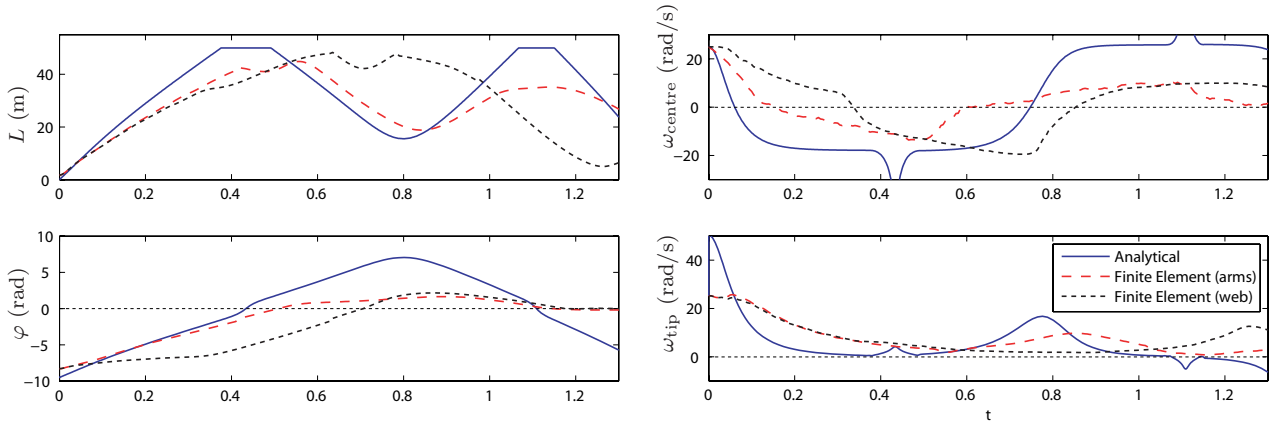


Figure 6. Free deployment of space web.

different deployments almost coincide. The deployment is initiated by an initial rotational velocity of 8π rad/s on the hub and the web. The star arms are coiled off from the hub, but then coiled on the centre hub again. The agreement between the two models is rather good for the length of the deployed arm, but not for the rotational velocities because the arms are not straight in the FE model.

Controlled deployment of star arms

A stable deployment can be achieved by applying the torque in Eq. (3), Figure 7. To model this in LS-DYNA feedback from the computed values is necessary. This is possible in the object version of LS-DYNA,³³ but was not implemented in the present study.

It was observed that the applied torque is unrealistically high. Hedgepeth used a torque approximately equal to 200 Nm in the simulations of the LOFT.²² To achieve a stable deployment with applied moments of the same order, the deployment velocity must be considerably lower than here. In reality the hub is smaller, which of course gives lower deployment velocity for a given rotational velocity. Alternatively, it is possible to decrease the initial rotational velocity.

Using a hub with radius 1 m and torque equal to $60\pi \approx 200$ Nm in the analytical model, the deployment characteristics shown in Figure 8 were obtained for different initial rotational velocities ω_0 . It is evident that for increased ω_0 , i.e. increased deployment velocity, the deployment is more difficult to control. The remedy is to use a greater torque.

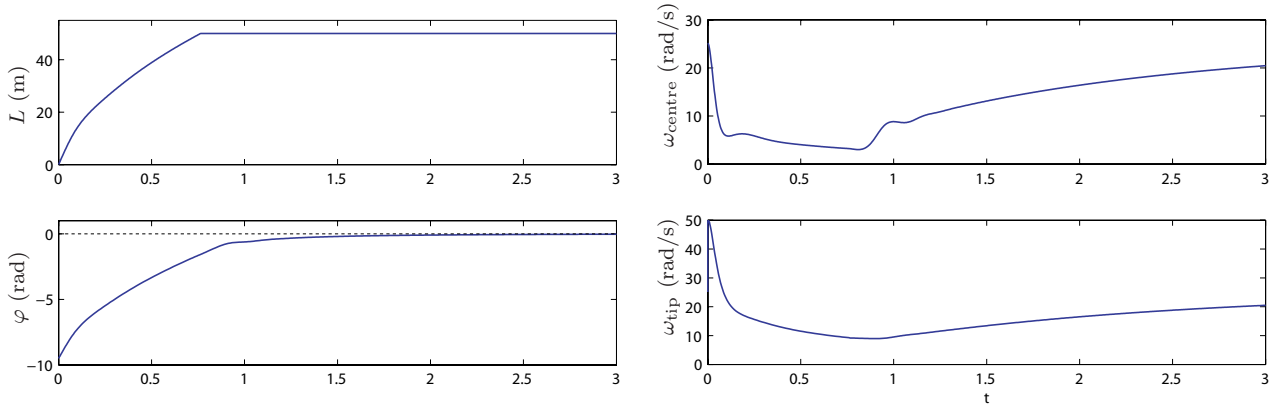


Figure 7. Deployment of space web using the control law in Eq. (3) with $M_0 = \omega_0 \cdot 10^5$.

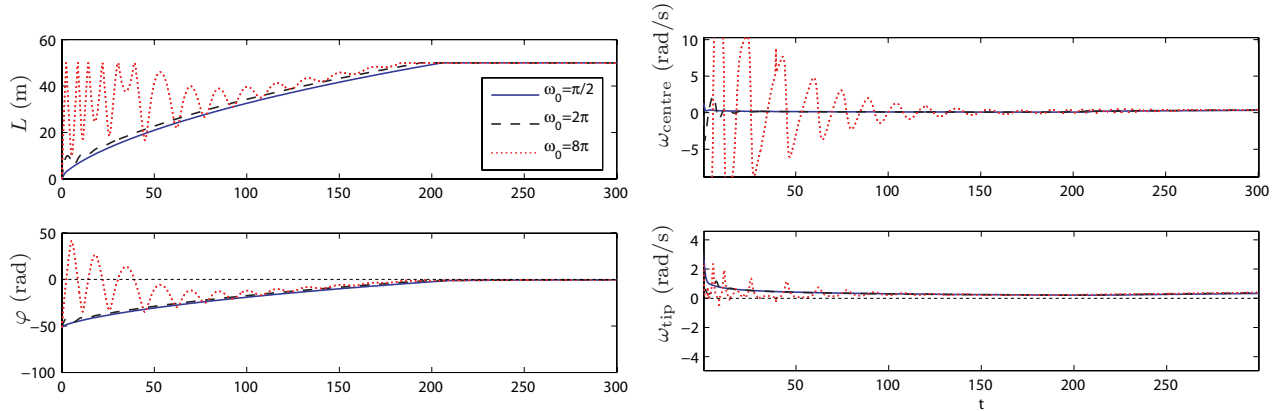


Figure 8. Deployment of the star arms. A torque is applied according to the control law in Eq. (3) with $M_0 = 60\pi$ Nm and $\omega_0 = \pi/2, 2\pi, 8\pi$ rad/s.

Rotational velocity according to Salama *et al.*

Salama *et al.*¹³ propose linearly increasing angular velocity of the inner hub, from 0 at time $t = 0$ to ω_{\max} at time $t = \Delta t$, and then keep the angular velocity constant at ω_{\max} . There is no systematic way to choose these parameters, but use of the values $\omega_{\max} = 8\pi$ rad/s and $\Delta t = 2$ s,¹³ resulted in the deployment in Figures 9 and 10. The arms are coiled off the centre hub, and not coiled back on the hub again. However, there are undesirable oscillations in the plane of rotation.

This example was also used to validate the analytical model. When a material that is 1000 times stiffer than Zylon[®] is used, the results from the analytical and finite element models are almost identical.

IX. Conclusions

The main conclusions from the present study are:

- Only a web with a quadratic mesh topology can be adequately prestressed by spinning.
- The star folding pattern makes it possible to deploy the web in two distinctive stages to achieve better control.
- The star folding pattern is advantageous from a modelling point of view since it can be described with simple equations.
- For the second deployment stage, coiling the arms around the hub was chosen in favour of a radial zig-zag scheme. The coiling scheme does not require additional tethers to control the deployment rate of the star arms, which is required in the zig-zag scheme.

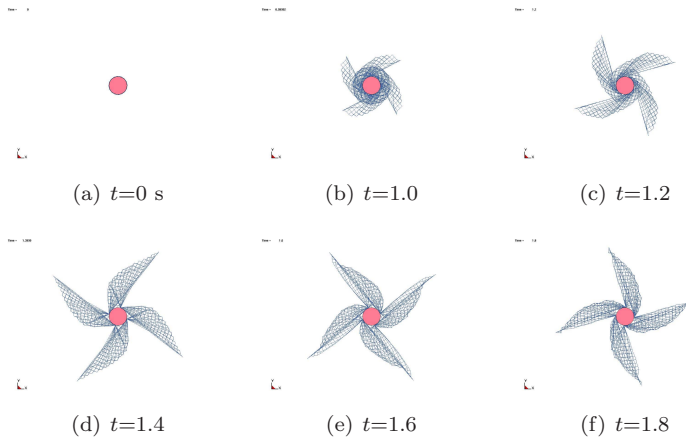


Figure 9. Deployment of a space web with rotational velocity varying linearly from 0 at $t = 0$ to 8π rad/s at 2 s.

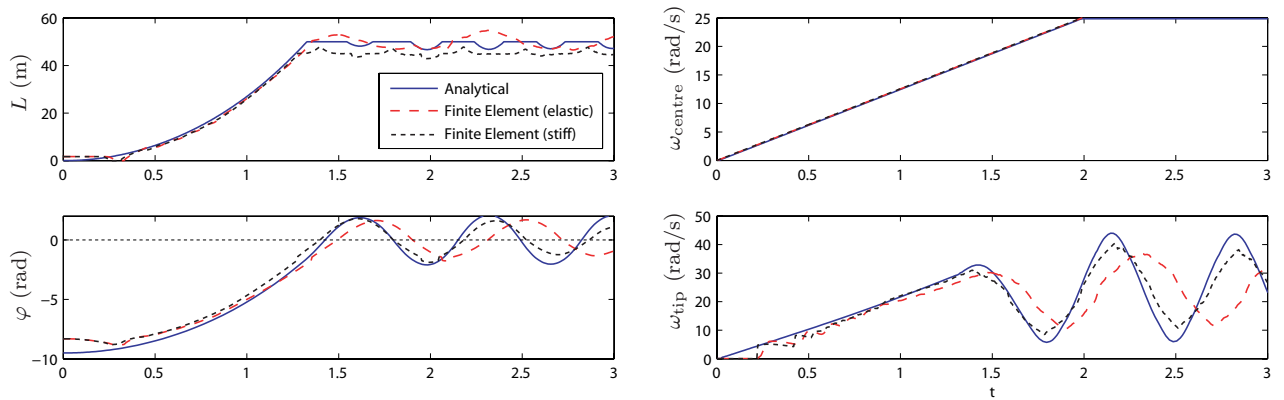


Figure 10. Deployment of a space web with rotational velocity varying linearly from 0 at $t = 0$ to 8π rad/s at 2 s.

- An analytical model, originally developed by Melnikov and Koshelev²⁰ and then slightly modified, and a finite element model implemented in LS-DYNA have been developed.
- The analytical and the finite element models produce almost identical results when the arms are straight, i.e. when energy is transferred from the hub to the arms, and a stiff material is used, i.e. no elasticity is involved. When material data for Zylon[®] is used, then the deployment is still similar, but different oscillatory behaviour occurs after the arms have been fully deployed.
- Both the analytical and finite element models show that free deployment is not possible.
- To stabilise the deployment, a torque can be applied to the central hub. The torque control law implies that the moment increases when the angular velocity of the hub decreases and vice versa. However, greater maximum moment is required if higher deployment velocity is desired.

References

- ¹S. Nakasuka, T. Aoki, I. Ikeda, Y. Tsuda, and Y. Kawakatsu. “Furoshiki Satellite”—a large membrane structure as a novel space system. *Acta Astronautica*, 48(5–12):461–468, 2001.
- ²S. Nakasuka, R. Funase, K. Nakada, N. Kaya, and J. C. Mankins. Large membrane “Furoshiki Satellite” applied to phased array antenna and its sounding rocket experiment. *Acta Astronautica*, 58:395–400, 2006.
- ³S. Nakasuka, T. Funane, Y. Nakamura, Y. Nojira, H. Sahara, F. Sasaki, and N. Kaya. Sounding rocket flight experiment for demonstrating “Furoshiki Satellite” for large phased array antenna. *Acta Astronautica*, 59:200–205, 2006.

- ⁴N. Kaya, M. Iwashita, S. Nakasuka, L. Summerer, and J. Mankins. Crawling robots on large web in rocket experiment on Furoshiki deployment. In *Proc. 55th Int. Astronomical Congress*, Vancouver, Canada, 4–8 October 2004. IAC-04-R3.
- ⁵S. Nakasuka and N. Kaya. Quick release on experiment results of mesh deployment and phased array antenna by S-310-36, September 4 2006. Online Internet: <http://www.isas.ac.jp/e/forefront/2006/nakasuka/>.
- ⁶G. Tibert and M. Gärdsback. Space webs, final report. Technical report, ESA, 2006. Ariadna ID: 05/4109, Contract Number: 19702/06/NL/HE.
- ⁷D. McKenzie, M. Cartmell, G. Radice, and M. Vasile. Space webs, final report. Technical report, ESA, 2006. Ariadna ID: 05/4109, Contract Number: 4919/05/NL/HE.
- ⁸H. U. Schuerch and R. MacNeal. Deployable centrifugally stabilized structures for atmospheric entry from space. NASA Contractor Report, NASA CR-69, July 1964.
- ⁹H. U. Schuerch and J. M. Hedgepeth. Large low-frequency orbiting radio telescope. NASA Contractor Report, NASA CR-1201, October 1968.
- ¹⁰W. M. Robbins, Jr. The feasibility of an orbiting 1500-meter radio telescope. NASA CR-792, Astro Research Corporation, 1967.
- ¹¹A. C. Kyser. Uniform-stress spinning filamentary disk. *AIAA Journal*, 3(7):1313–1316, 1965.
- ¹²R. H. MacNeal. The Heliogyro: an interplanetary flying machine. Astro Research Corporation, ARC-R-249, March 1967.
- ¹³M. Salama, C. White, and R. Leland. Ground demonstration of a spinning solar sail deployment concept. *Journal of Spacecraft and Rockets*, 40(1):9–14, 2003.
- ¹⁴R. L. Burton, V. L. Coverstone, J. Hargens-Rysanek, K. M. Ertmer, T. Botter, G. Benavides, B. Woo, D. L. Carroll, P. A. Gierow, G. Farmer, and J. Cardin. UltraSail — ultra-lightweight solar sail concept. In *Proc. 41st AIAA/ASME/SAE/ASEE Joint Propulsion Conf.*, Tucson, AZ, USA, July 10–13 2005. AIAA-2005-4117.
- ¹⁵J. Mitsugi, M. Natori, and K. Miura. Preliminary evaluation of the spinning solar sail. In *Proc. 28th AIAA/ASME/ASCE/AHS/ASC Structures, Structural Dynamics, and Materials Conf.*, Monterey, CA, USA, April 1987. AIAA-1987-742.
- ¹⁶S. Matunaga, H. Yabe, K. Nakaya, M. Iai, K. Omagari, and O. Mori. Membrane deployment for spinning formation-flight solar sail. In *Proc. 14th Workshop on Astrodynamics and Flight Mechanics*, Tokyo, July 26–27 2004. Paper A-11.
- ¹⁷O. Mori, Y. Tsuda, Y. Nishimura, and J. Kawaguchi. Deployment dynamics of clover type solar sail. In *Proc. 14th Workshop on Astrodynamics and Flight Mechanics*, Tokyo, July 26–27 2004. Paper A-5.
- ¹⁸S. Masumoto, K. Omagari, T. Yamanaka, and S. Matunaga. System configuration of tethered spinning solar sail for orbital experiment: numerical simulation and ground experiment. In *Proc. 25th International Symposium on Space Technology and Science (ISTS)*, Kanazawa City, Japan, June 4–11 2006. Paper D-21.
- ¹⁹Y. Tsuda, K. Nakaya, O. Mori, and T. Yamamoto. Microsatellite-class solar sail demonstrator — mission design and development status. In *Proc. 25th International Symposium on Space Technology and Science (ISTS)*, Kanazawa City, Japan, June 4–11 2006. Paper K-37.
- ²⁰V. M. Melnikov and V. A. Koshelev. *Large space structures formed by centrifugal forces*, volume 4 of *Earth Space Institute Book Series*. Gordon and Breach Science Publishers, India, 1998.
- ²¹G. B. Palmerini, S. Sgubini, and M. Sabatini. Space webs based on rotating tethered formations. Valencia, Spain, 2006. 57th International Astronautical Congress, 2–6th October.
- ²²J. M. Hedgepeth. Dynamics of a large spin-stiffened deployable paraboloidal antenna. *Journal of Spacecraft and Rockets*, 7(9):1043–1048, 1970.
- ²³L. G. Seely, M. Zimmerman, and J. McLaughlin. The use of Zylon fibers in ULDB tendons. *Advances in Space Research*, 33:1736–1740, 2004.
- ²⁴J. W. S. Hearle, editor. *High-performance fibers*. Woodhead publishing, Cambridge, UK, 2001.
- ²⁵K. A. Gittemeier, C. W. Hawk, M. M. Finckenor, and E. Watts. Space environmental effects on coated tether materials. In *Proc. 41st AIAA/ASME/SAE/ASEE Joint Propulsion Conf.*, Tucson, AZ, USA, 10–13 July 2005. AIAA-2005-4433.
- ²⁶S. Pellegrino. Structural computations with the singular value decomposition of the equilibrium matrix. *International Journal of Solids and Structures*, 30(21):3025–3035, 1993.
- ²⁷G. Tibert. *Deployable Tensegrity Structures for Space Applications*. PhD thesis, Royal Institute of Technology, Stockholm, Sweden, 2002.
- ²⁸W. M. Robbins, Jr. Spinning paraboloidal tension networks. NASA CR-873, Astro Research Corporation, 1967.
- ²⁹K. Miura. Method of packaging and deployment of large membranes in space. In *Proc. 31st Int. Astronautical Congress*, Tokyo, 21–28 September 1980. IAF-80-A31.
- ³⁰S. D. Guest and S. Pellegrino. Inextensional wrapping of flat membranes. In R. Motro and T. Wester, editors, *Proc. 1st Int. Conf. on Structural Morphology*, pages 203–215, Montpellier, France, 7–11 September 1992.
- ³¹H. W. Scheel. Space-saving storage of flexible sheets. United States Patent, US 3,848,821, November 19, 1974.
- ³²H. Furuya, Y. Inoue, and T. Masuoka. Concept and deployment characteristics of rotationally skew fold membrane for spinning solar sail. In *Proc. 14th Workshop on Astrodynamics and Flight Mechanics*, Tokyo, July 26–27 2004. Paper A-3.
- ³³Livermore software technology corporation, Livermore, CA, USA. *LS-DYNA Keyword user's manual, version 970*, April 2003.
- ³⁴T.J.R. Hughes, R.L. Taylor, J.L. Sackman, A.C. Curnier, and W. Kanoknukulchai. A finite element method for a class of contact-impact problems. *Comput. Methods Appl. Mech. Engrg.*, 8:249–276, 1976.